Dear Author,

Here are the proofs of your article.

- You can submit your corrections **online**, via **e-mail** or by **fax**.

- For **online** submission please insert your corrections in the online correction form. Always indicate the line number to which the correction refers.

- You can also insert your corrections in the proof PDF and **email** the annotated PDF.

- For fax submission, please ensure that your corrections are clearly legible. Use a fine black pen and write the correction in the margin, not too close to the edge of the page.

- Remember to note the **journal title**, **article number**, and **your name** when sending your response via e-mail or fax.

- **Check** the metadata sheet to make sure that the header information, especially author names and the corresponding affiliations are correctly shown.

- **Check** the questions that may have arisen during copy editing and insert your answers/corrections.

- **Check** that the text is complete and that all figures, tables and their legends are included. Also check the accuracy of special characters, equations, and electronic supplementary material if applicable. If necessary refer to the *Edited manuscript*.

- The publication of inaccurate data such as dosages and units can have serious consequences. Please take particular care that all such details are correct.

- Please **do not** make changes that involve only matters of style. We have generally introduced forms that follow the journal's style.
  Substantial changes in content, e.g., new results, corrected values, title and authorship are not allowed without the approval of the responsible editor. In such a case, please contact the Editorial Office and return his/her consent together with the proof.

- If we do not receive your corrections **within 48 hours**, we will send you a reminder.

- Your article will be published **Online First** approximately one week after receipt of your corrected proofs. This is the **official first publication** citable with the DOI. **Further changes are, therefore, not possible.**

- The **printed version** will follow in a forthcoming issue.

Please note

After online publication, subscribers (personal/institutional) to this journal will have access to the complete article via the DOI using the URL: http://dx.doi.org/[DOI].
If you would like to know when your article has been published online, take advantage of our free alert service. For registration and further information go to: http://www.link.springer.com.

Due to the electronic nature of the procedure, the manuscript and the original figures will only be returned to you on special request. When you return your corrections, please inform us if you would like to have these documents returned.

Metadata of the article that will be visualized in OnlineFirst

	ORCID	
Author	Family Name	**Bisio**
	Particle	
	Given Name	**C.**
	Suffix	
	Division	Department of Science and Technological Innovation
	Organization	University of Eastern Piedmont
	Address	Viale Teresa Michel 11, 15121, Alessandria, Italy
	Phone	
	Fax	
	Email	
	URL	
	ORCID	
Author	Family Name	**Gatti**
	Particle	
	Given Name	**G.**
	Suffix	
	Division	Department of Science and Technological Innovation
	Organization	University of Eastern Piedmont
	Address	Viale Teresa Michel 11, 15121, Alessandria, Italy
	Phone	
	Fax	
	Email	
	URL	
	ORCID	
Author	Family Name	**Coluccia**
	Particle	
	Given Name	**S.**
	Suffix	
	Division	Department of Chemistry
	Organization	University of Turin
	Address	Via P. Giuria 7, 10125, Torino, Italy
	Phone	
	Fax	
	Email	
	URL	
	ORCID	

Abstract	Porous carbons are materials of wide application and their request is more and more increasing in the last years: Properly designed synthesis is presently available for the preparation of materials to be used in the several fields (e.g.: adsorption, molecular separation, and catalysis). The characterization of the porous carbons is usually carried out using different techniques such as thermogravimetric analyses, Raman spectroscopy, Scanning electron microscopy, etc. In this work, the micro-Raman technique is adopted in

combination with N_2 physisorption at 77 K to monitor how the synthetic approach influences the presence of either amorphous or ordered regions in porous carbons. The typical D and G Raman bands of activated carbons have been carefully deconvoluted in six different components by a fitting procedure, and the determined $R_1 = I_{D1}/I_G$ ratio correlated to their specific surface area.

1 **On the correlation between Raman spectra**
2 **and structural properties of activated carbons derived**
3 **by hyper-crosslinked polymers**

4 **A. Croce[1] · G. Re[2] · C. Bisio[1] · G. Gatti[1] · S. Coluccia[3] · L. Marchese[1]**

7 **Abstract**
8 Porous carbons are materials of wide application and their request is more and more
9 increasing in the last years: Properly designed synthesis is presently available for the
10 preparation of materials to be used in the several fields (e.g.: adsorption, molecular
11 separation, and catalysis). The characterization of the porous carbons is usually car-
12 ried out using different techniques such as thermogravimetric analyses, Raman spec-
13 troscopy, Scanning electron microscopy, etc. In this work, the micro-Raman tech-
14 nique is adopted in combination with N_2 physisorption at 77 K to monitor how the
15 synthetic approach influences the presence of either amorphous or ordered regions
16 in porous carbons. The typical D and G Raman bands of activated carbons have
17 been carefully deconvoluted in six different components by a fitting procedure, and
18 the determined $R_1 = I_{D1}/I_G$ ratio correlated to their specific surface area.

21 **Introduction**

22 In the last years, the demand of new porous materials has rapidly increased in
23 relation to the application in different fields, such as air and water decontamina-
24 tion, gas and fuel storages, molecular separation, catalysis, etc. [1–4]. Syntheses

A3 ✉ L. Marchese
A4 leonardo.marchese@uniupo.it

A5 1 Department of Science and Technological Innovation, University of Eastern Piedmont, Viale
A6 Teresa Michel 11, 15121 Alessandria, Italy

A7 2 National Institute of Geophysics and Volcanology, Via Cesare Battisti 53, 56125 Pisa, Italy

A8 3 Department of Chemistry, University of Turin, Via P. Giuria 7, 10125 Torino, Italy

| Journal : **SmallExtended 11164** | Article No : **4338** | Pages : **13** | MS Code : **4338** | Dispatch : **9-12-2020** |

A. Croce et al.

25 of porous materials are designed in order to obtain materials that satisfy specific
26 requirements for their final application. In particular, desired physical character-
27 istics as high specific surface area, pore dimensions and volume are essential for
28 adsorption [5–8], molecular separation [9–11] and catalysis [12–14]. Nowadays,
29 various classes of porous materials with different chemical compositions have
30 been developed, among which inorganic zeolites and synthetic clays (bentonite,
31 montmorillonite), organic–inorganic hybrid frameworks (e.g., metal–organic
32 frameworks MOFs) [15–17], covalent-organic frameworks (COFs) possibly with
33 heteroatoms [18], porous organic polymer (POP) [19, 20] and activated carbons
34 (ACs) [21–25].

35 The POP includes different types of material, and among these the porous aro-
36 matic frameworks (PAFs) and hyper-crosslinked polymers (HCPs) families have
37 received great attention in relation to their peculiar properties such as high pore
38 volume (tunable from micro- to meso-porosity) and physico-chemical stability
39 (especially in aqueous environment) and shows the possibility to perform com-
40 positional control during their synthesis: using different linkers it is possible to
41 obtain a large number of different porous structures and modulate the hierarchical
42 porosity [26–36].

43 A wide family of porous materials that has been investigated for decades is
44 that of carbonaceous solids, obtained by carbonization of biomass [37–39],
45 though the use of raw materials with not constant chemical composition leads
46 to the preparation of activated carbon whose physico-chemical properties are not
47 completely controllable.

48 One strategy to overcome this problem is the use of polymers as raw materials
49 [40], and adopting selected physical or chemical activations [41, 42]. In addi-
50 tion, these materials are very simple to synthesize, and the costs of production are
51 lower than other materials [43].

52 Many examples of this strategy, such as the use of HCPs for the preparation of
53 microporous carbonaceous materials, can be found in the recent literature [44].

54 A key point is the subsequent phase of characterization to have a clear under-
55 standing of the properties of the materials, and it is not straightforward to relate
56 the information obtained from different techniques. A correlation between
57 Raman analyses and the porosimetric properties of carbons could be a valid and
58 rapid alternative to the use of other techniques and be used as a methodological
59 approach in the selection of the most promising materials. Moreover, the Raman
60 technique does not need any particular manipulation of the samples, avoiding
61 material modifications consequent to the preparation steps prior the analyses.

62 Using this approach, we have performed micro-Raman spectroscopy analyses
63 for the characterization of porous carbons obtained by HCPs prepared with dif-
64 ferent ratios of precursors (tetraphenylmethane (TPM) and formaldehyde dime-
65 thyl acetal (FDA)), and subsequently carbonized in three different ways [44]. The
66 Raman spectra are elaborated with a specific fitting deconvolution process, aim-
67 ing at acquiring information on the material structures, in order to assess the level
68 of amorphous *vs* crystalline components. These data are subsequently paired with
69 textural properties (e.g., specific surface area) of studied materials.

Materials and methods

Synthesis of HCP materials (UPO) and post-synthesis treatments (KUPO)

The HCP materials have been synthesized by using procedure already described elsewhere [44]. The hyper-crosslinked polymers (UPO) were prepared using ferric chloride (Sigma Aldrich, quality level MQ 200) and tetraphenylmethane (TPM 97%; Sigma-Aldrich) suspended in dichloroethane (DCE 99.8%; Sigma-Aldrich), stirred at room temperature until a homogeneous thick gel was obtained.

Formaldehydedymethylacetal (FDA, Sigma-Aldrich, quality level MQ 200) was added drop-wise, to the thick gel under stirring, then heated under reflux, diluted in ethanol after cooling to room temperature, washed until neutral pH, and finally dried in oven at 100 °C. The reaction was carried out using two different TPM:FDA molar ratios of 1:8 and 1:16, respectively.

Different procedures of chemical activation based on thermal and chemical treatments have been subsequently used to modify the contact between the activating agent (KOH) and the polymers matrix. In particular, three different activation procedures were followed: (1) in the pre-activation method 1 a solid solution of UPO material and KOH (ratio 1:3) is prepared under inert conditions; (2) in the pre-activation method 2 a solid solution of UPO and KOH (ratio 1:3) is prepared in air for 5 h in order to allow ambient water hydrating KOH thus facilitating dissolution into the UPO material and (3) in the pre-activation method 3 UPO material is stirred in a solution of KOH (1 M) in ethanol for 18 h, and subsequently dried under vacuum at 50 °C.

After the preparation, these mixtures were heated to 750–800 °C, and subsequently hold under isothermal conditions for 1 h. The carbonaceous materials obtained by these procedures were labeled as ACx-y–z, where x refers to the pre-activation method, y indicates the TPM:FDA ratio of the parent polymer and z the activation temperature. The obtained samples are listed in Table 1.

Table 1 Synthesis procedure of the samples analyzed in this work

Sample name	Pre-activation method	TPM:FDA molar ratio	Heating (°C)
AC1-8–750	KOH (1:3) inert	1:8	750
AC1-8–800	KOH (1:3) inert	1:8	800
AC1-16–800	KOH (1:3) inert	1:16	800
AC2-8–750	KOH (1:3) air	1:8	750
AC2-8–800	KOH (1:3) air	1:8	800
AC2-16–800	KOH (1:3) air	1:16	800
AC3-8–800	KOH (1 M) ethanol (18 h)	1:8	800
AC3-16–750	KOH (1 M) ethanol (18 h)	1:16	750

Characterization techniques

The synthesized powders were analyzed by micro-Raman spectroscopy, using a JobinYvon HR800 LabRam µ-spectrometer (HORIBA JobinYvon, Paris, France). The spectra were collected at room temperature, addressing the laser beam onto the samples thanks to the annexed Optical Microscope (OM; Olympus BX41; Olympus, Tokyo, Japan). The instrument was equipped with a HeNe 20 mW laser (wavelength 632.8 nm) and a charge-coupled air-cooled device detector. An instrument calibration was performed checking the position and intensity of the Si band at 520.65 ± 0.05 cm^{-1} before running each experimental acquisition. In order to obtain the best signal/noise ratio, every spectrum was obtained carrying out 30 exposures of 120 s for the 16 spectral ranges that cover the 3500–750 cm^{-1} (about 16 h) and where characteristic first- and second-order bands of the carbonaceous materials (CMs) lie [45–49]. No filter was applied to the signal for spectra acquisitions, after the checking that no sample modification was observed addressing a full power beam. Spectra were also acquired by a JobinYvon Evolution micro-Raman spectrometer (HORIBA JobinYvon, Paris, France), equipped with a Nd:YAG laser source (wavelength 532 nm). Autocalibration of the instrument was carried out before every experimental session, using the ~ 520.6 cm^{-1} band of Si. The spectra were acquired addressing 3.2% of the laser power on the materials, with 2 exposures of 30 s: this experimental setting allowed obtaining good spectra and no sample modifications under laser energy.

In order to exclude sample modification under green laser, different times and excitation source powers have been applied to carry out sample characterization. Applying a longer time or a higher power, it was evident sample modification during analyses, observing both Raman patterns and optical modifications of the samples after spectral acquisitions.

A fitting procedure was performed using the package software of the OPUS V. 5.5 on the first-order CM bands, with different runs in order to obtain the minimal residual error, considering six different components (five Lorentzian bands, G, D1, D2, D4, and D5 one Gaussian band, D3) after baseline subtraction of the fluorescence effect. The obtained results were utilized to calibrate an automatic 6-way fitting process using Fityk V. 0.9.8 software in order to maintain the same operational procedure in spectrum elaborations and minimize artificial variations. This process was set using a compiled script aimed at the automatic recognition of five Lorentzian and one Gaussian (D3) bands. The script firstly fits D and G bands, then searches at the same time D2 and D3 bands and finally recognizes the last two bands centered at about 1270 and 1150 cm^{-1} (D4 and D5 bands). All the obtained results were compared with the manual fitting process performed using OPUS software.

The N_2 physisorption measurements were carried out at 77 K in the relative pressure (P/P0) range 1×10^{-7}–1 by using an Autosorb iQ/ASiQwin instrument (Anton Paar QuantaTec Inc., Boynton Beach, FL, USA). Prior to the analysis, the samples were outgassed at 150 °C for 16 h (residual pressure lower than 10^{-6} Torr). The apparent BET surface areas were calculated over a relative pressure range recommended by the "Micropore BET Assistant", a program that is implemented in ASiQWin Quantachrome software to facilitate the selection points within the linear

142 range of the BET plot for microporous materials. The pore size distribution for all
143 samples is calculated using quenched solid density functional theory (QSDFT) on
144 a carbon surface with slit/cylindrical geometry applied to the adsorption branch
145 (method with the smallest fitting error).

Results

147 Micro-Raman spectroscopy was applied to the activated carbons (ACs) synthesized
148 from hyper-crosslinked polymers (HCPs) reported in Table 1. The characteristics D
149 and G bands, each of them being composite of several components, were always
150 observed (Fig. 1).
151 Deconvolution process was performed to extract the single components, which
152 were tentatively correlated to the specific surface area of the synthesized samples.
153 An automatic six-way fitting applied by means of the Fityk software was optimized
154 in order to determine the ratio between the intensity of D1 (disorder band) and G
155 (graphitic band) (R_1), obtained from the spectra acquired by the two laser sources
156 as proposed by Beyssac et al. in 2002. [46]. A third fully automated method (IFORS
157 software) was applied to further validate the manual and the semiautomatic fitting
158 processes (data not shown), in particular to check the position of the baseline used
159 for background subtraction and peak positions.
160 On the synthesized materials, by using red and green laser sources two different
161 shapes of the first-order Raman bands were observed. Figure 1a refers to the data
162 obtained with the laser at 632.8 nm, whereas Fig. 1b to spectra acquired with the
163 laser at 532 nm wavelength.
164 Finally, two examples of first-order band fitting are reported in Fig. 2a, b high-
165 lighting peak position and band labels.
166 The D1 band at about 1330 cm^{-1} is due to defective sp^3 carbon: The intensity
167 and position of this band depend on the presence of amorphous regions in the
168 carbon materials. Conversely, the intensity of bands at 1550–1580 cm^{-1} (G band)
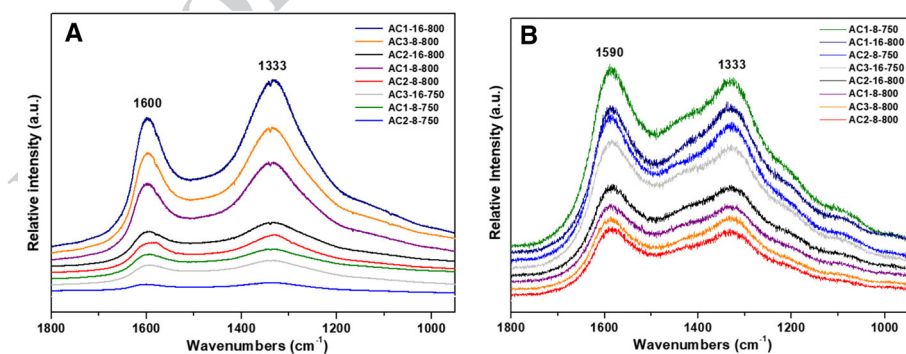

Fig. 1 Representative Raman spectra obtained on ACs samples. **a** Raman spectra obtained by 632.8 nm laser source; **b** Raman spectra obtained by 532 nm laser source
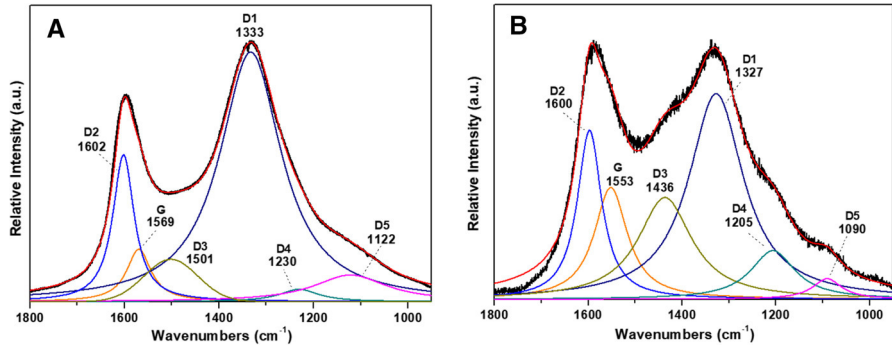
Fig. 2 Example of spectrum fitting of the sample AC1-16–800 with 632.8 nm laser source **a** and 532 nm laser source; **b**; above the band position values, the labels of the six obtained bands are reported

169   is related to the extension of ordered regions [50]. The D1 band is strictly related
170   to that lying between 1600 and 1615 cm^{-1}, called D2 band.

171   These bands are relevant to estimate the disorder degree in carbonaceous struc-
172   tures, and accurate best fitting evaluations are needed to obtain reliable informa-
173   tion. In addition, other three bands lie in the 1500–1000 cm^{-1} range: the band
174   at around 1500 cm^{-1} is reported in the literature as D3, while the band at about
175   1230–1200 cm^{-1} is called D4, and the last at about 1100–1120 cm^{-1} is called D5.

176   Different numbers of bands in this spectral range are reported in the literature,
177   and this confirms that the study of carbon materials using Raman features is not
178   yet univocally made. For the sake of simplicity and clarity the bands nomencla-
179   ture is reported onward in this work [45–61].

180   Automatic fitting method was validated comparing the obtained R_1 ratios
181   where the R_1 is the intensity ratio between D1 and G bands:

$$R_1 = \frac{I_D}{I_G} \tag{1}$$

184   Small R_1 values indicate that the material is characterized by a greater struc-
185   tural order: When the carbon is more crystalline, the G band shows higher inten-
186   sity in comparison to the D1.

187   Data obtained by the fitting process and the calculated R_1 ratios are reported in
188   Tables 2 (red laser source) and 3 (green laser source).

189   The R_1 obtained by the two laser sources were related to the values of SSA
190   [44] obtained by physisorption analysis of nitrogen at 77 K (Fig. 3, and Tables 2
191   and 3).

192   The highest R_1 values are obtained on samples AC1-16–800, AC3-8–800, AC1-
193   8–800 and AC2-16–800 using red laser source. This trend is confirmed by the data
194   obtained using green laser. The first two samples show also the highest values of
195   V_{Total} and V_{micro}, while V_{meso} values are low (<0.3 cm^3/g). The AC-3-8–800 sample
196   has a high V_{Total}, but the lowest SSA (<2400 m^2/g) and V_{micro} (<0.7 cm^3/g), and
197   also the highest V_{meso} among the studied samples (>0.5cm^3/g). The samples AC1-
198   8–800 and AC2-16–800, as AC1-16–800, have high SSA and V_{micro} and low V_{meso}.

Table 2 Band parameters obtained from Raman spectra acquired with 632.8 nm laser source applying the automatic fitting procedure described in the experimental section

Sample	R_1[a]	R_2[b]	FWHM[c] D1 [cm^{-1}]	FWHM[c] D2 [cm^{-1}]	Pos.[d] D [cm^{-1}]	Pos.[d] G [cm^{-1}]	Diff. G-D [cm^{-1}]	SSA [m^{2}g^{-1}]
AC1-8–750	1.88	0.78	119.78	46.01	1340	1576	236	2562
AC1-8–800	2.30	0.74	133.23	43.44	1341	1583	242	2666
AC1-16–800	2.39	0.76	148.49	43.02	1337	1577	240	2950
AC2-8–750	1.79	0.65	142.68	47.06	1336	1589	253	2500
AC2-8–800	1.60	0.68	118.64	42.85	1333	1579	246	2400
AC2-16–800	2.25	0.70	127.33	48.28	1340	1578	238	2700
AC3-8–800	2.35	0.75	134.69	42.59	1340	1582	242	2975
AC3-16–750	2.38	0.66	145.28	59.92	1345	1560	215	2318

[a]$R_1 = I_{D1}/I_G$

[b]$R_2 = $ area $[D1/(G + D1 + D2)]$

[c]FWHM = Full Width at Half Maximum

[d]Pos. = Band position
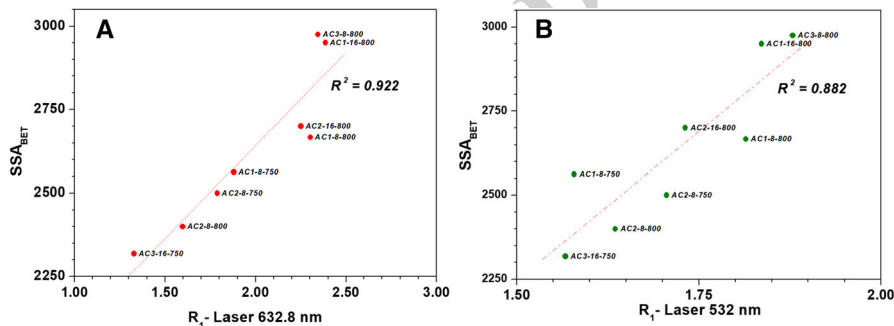
Fig. 3 **a** R_1 ratio obtained by red laser source versus SSA-BET data; **b** R1 ratio obtained by green laser source versus SSA-BET data

As discussed in the following section, the obtained data show a linear correlation between R_1 and SSA.

Discussion

During the last decades, it has been demonstrated that micro-Raman spectroscopy is a powerful tool in ACs characterization, in particular for the order/disorder and defects definition. Raman spectra of ACs are, at first sight, defined by a peculiar

Table 3 Band parameters obtained from Raman spectra acquired with 532 nm laser source applying the automatic fitting procedure described in the experimental section

Sample	R_1[a]	R_2[b]	FWHM[c] D1 [cm^{-1}]	FWHM[c] D2 [cm^{-1}]	Pos.[d] D [cm^{-1}]	Pos.[d] G [cm^{-1}]	Diff. G-D [cm^{-1}]	SSA [m^{2}g^{-1}]
AC1-8–750	1.58	0.57	139.22	62.08	1327	1553	226	2562
AC1-8–800	1.81	0.58	140.43	64.66	1327	1549	222	2666
AC1-16–800	1.84	0.59	141.61	62.84	1327	1552	225	2950
AC2-8–750	1.70	0.58	137.39	60.25	1327	1553	226	2500
AC2-8–800	1.63	0.59	143.84	61.06	1328	1555	227	2400
AC2-16–800	1.73	0.58	142.24	63.99	1325	1550	225	2700
AC3-8–800	1.89	0.59	131.71	59.22	1327	1552	225	2975
AC3-16–750	1.57	0.56	141.99	63.60	1325	1551	226	2318

[a]$R_1 = I_{D1}/I_G$

[b]$R_2 = $ area [D1/(G + D1 + D2)]

[c]FWHM = Full Width at Half Maximum

[d]Pos. = Band position

spectral feature, formed by first- and second-order vibrations [46–49]. The intensity ratio among these bands, and in particular the one between D and G intensities (R_1) is an important parameter related to the carbon organization in the samples [57].

The works in literature proved that 514 or 532 nm wavelengths give the best signal/noise ratio in ACs characterization [54]. In fact, these laser sources give Raman spectra with relative low fluorescence effects in the range where the ACs bands lie, allowing band fitting with minor errors in the obtained band parameters than from results derived by red lasers. Nevertheless, the excitation energy of green laser sources is generally more powerful, and they might modify ACs during the analyses. For this reason, in this work, two different laser sources were used in AC characterization for the determination of spectroscopic parameters.

Several works studied adopted different best fitting procedures to deconvolute the components of the two more intense bands constantly present in all AC spectra and proposed a series of equations to calculate disorder/order ratios [46, 48, 51, 55, 56]. The different approaches extracted a variable number of components as a result of the fitting process, thus providing a great variability in band names and mathematical methods. In Table 4 and SI1 the band labelling in several referenced papers are listed. One of the most crucial variables is the number of components by which the deconvolution process is made; a second one is the type of fitted band (e.g.: Gaussian, Lorentzian, Voigt) [59, 62].

From the data reported in Tables 4 and SI1 it is clear that the number and name of the fitted bands vary from one study to another. In this work the best fitting process, i.e., that with the minimum residual error, adopted a six-way fitting and the deconvoluted bands were named G, D1, D2, D3, D4, and D5. The R_1 values obtained from

Table 4 List of Raman studies of carbonaceous materials where the bands in the 1800–900 cm^{-1} spectral range have been deconvoluted and classified

Laser wavelength	Name and position (cm^{-1}) of the C bands						Reference
	G	D1	D2	D3	–		
514 nm + 532 nm	G	D1	D2	D3	–	–	[46]
514, 633, 780 nm	G~1580	D1 (D)~1350	D2 (D')~1620	D3 (D''; A)>1500	D4 (I)~1200	–	[49]
514 nm	G	D1	D2	D3	D4	–	[62]
488 nm	G~1580	D1~1350	D2~1620	D3~1500	D4~1250	–	[59]
457, 514, 633, 752 nm	G	D	D'	D3	D4	–	[51]
266, 532, 633, 785 nm	G~1580	D variable by laser	D' variable by laser	A~1530	TPA variable by laser	–	[55]
532 nm	G~1585	D~1350	D''not indicated, ~1610	D*1500–1550	D*1150–1200	–	[53]
514, 632 nm	G	D	D'	D3~1438	D2~1260	D1~1185	[60]
532 nm	G~1585	D~1350	D''not indicated	D''1500–1550	D*1150–1200	–	[58]
532 nm	G	D1	D2	D3	D4	–	[61]
473 nm	G1610–1570	D1350	G$_R$1500–1570	D31450–1500	S1100–1200	S$_L$~1250	[52]
–	G	D	D'	D3	D4	D5	[45]
532, 632.8 nm	G	D1	D2	D3	D4	D5	This work

The data obtained in this work are reported for comparison

*a band at 1700 is assigned to the presence of C=O groups

229 the fitted first-order bands, when compared to the SSA data, provided a first impor-
230 tant information about the disorder degree of the ACs structures. In fact, R_1 shows
231 medium–high values when the measured SSA are medium–high (Table SI1): despite
232 the limited variability of these parameters, and their completely different experimen-
233 tal nature, a linear relationship between R_1 and SSA can be inferred. The reason for
234 this is that both parameters are correlated with the structural/morphological nature
235 of the carbons under study. High R_1 values are related, in fact, to a more extended
236 disorder inside the AC materials and it is highly possible that disordered carbons
237 display high specific surface area (SSA), as proposed by Roh et al. [63] on Activated
238 Carbon Fibers (ACFs).

239 Finally, as far as the polymer carbonization at high temperature is con-
240 cerned, it should be noticed that it occurs in the presence of KOH activation
241 agent as a solid–solid/solid–liquid reaction [64], according to the general Eq. 6
242 $KOH + 2C \rightarrow 2\ K + 3H_2 + 2K_2CO_3$. Moreover, when the activation temperature
243 increases at above 700 °C, the K_2CO_3 produced by the reaction starts to decom-
244 pose into K_2O and CO_2. The high microporosity in the carbon matrix is formed due
245 to the triple effects of chemical activation, physical activation, and the expansion
246 of the carbon lattices by metallic potassium intercalation: All these effects lead to
247 microporous carbons with very high SSA.

Conclusions

249 From the obtained results, it is found that micro-Raman data, considering the whole
250 series of parameters obtained by fitting process of the first-order bands, are related to
251 specific surface area of AC materials. In particular, among the considered calculated
252 Raman parameters, a linear relationship between R_1 (I_{D1}/I_G) and SSA-BET values
253 can be proposed. The correlation has been proved using as excitation sources for **AQ2**
254 Raman spectra both 632.8 and 532 nm laser wavelengths, and this suggests that not
255 significant structural variations occur during the prolonged exposure (16 h) under
256 the red laser source of samples here investigated. This result on porous carbons con- **AQ3**
257 firms the trend observed in the work of Roh et al., 2008, on activated carbon fibers
258 [63]. Further analyses should be carried out on a larger statistical significative num-
259 ber of samples to understand if this correlation may be predictive of physical charac-
260 teristics (especially SSA) of synthesized porous carbons, trying to calibrate Raman
261 spectroscopy as a method for this kind of studies.

A memory of Prof. Michel Che

263 I met Prof. Michel Che for the first time in Paris on 16 November 1988, when I was
264 a Ph.D. student under the supervision of Prof. Salvatore (Totò) Coluccia, one of his
265 best friends. I do remember clearly that moment because it was the first birthday of **AQ4**
266 my daughter Isabella, and I went to Paris with Totò and Prof. Adriano Zecchina for
267 the first meeting of a European project coordinated by Prof. Che. The memory of
268 that occasion is vivid, I collected the last IR spectra of CO adsorbed on Pt dispersed

Journal : **SmallExtended 11164** | Article No : **4338** | Pages : **13** | MS Code : **4338** | Dispatch : **9-12-2020**

On the correlation between Raman spectra and structural…

269 on TiO2, just one hour before catching the TGV for Paris, and during the travel
270 I completed the last slides. The excitation was very high because it was my first
271 experience abroad as PhD and I had to speak in front of famous persons, just known
272 reading the literature, Michel Che and Geoffrey Bond. Since that meeting I appreci-
273 ated the human qualities of Michel, as I used to name him more familiarly, his love
274 for science and his care for young scientists. During the last 30 years I met him sev-
275 eral times, and I have been always fascinated by his capacity of dialogue on life and
276 science, great remembrances are his conversations with Totò and sir John Meurig
277 Thomas, always ironic and full of jokes, beside relevant scientific issues. The legacy
278 of Michel on surface chemistry is invaluable, his open mind and humanity will live
279 forever in all people who had the pleasure to know him.
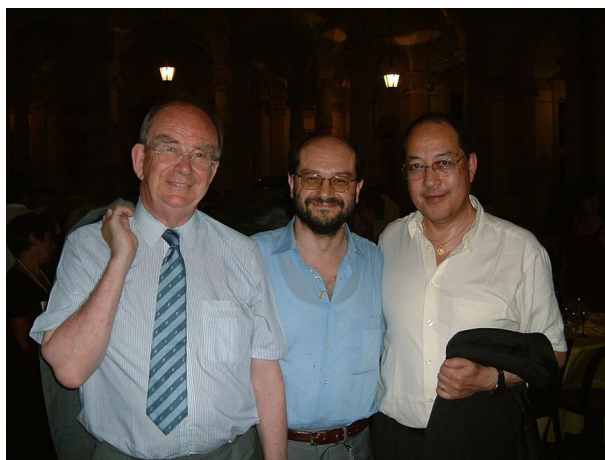
280
281 Photo: with Prof. Michel Che (right end), me (Prof. Leonardo Marchese) (center),
282 and Prof. Sir John M. Thomas (left end) in Torino in 2012.

References

287 1. M.D. Deanna, S. Berend, R.L. Jeffrey, Angew. Chem. Int. Ed. **49**, 6058 (2010)
288 2. W.M. Frota, J.A.S. Sa, S.S.B. Moraes, B.R.P. Rocha, K.A.R. Ismail, Energy Policy **38**, 3830 (2010)
289 3. I.P. Jain, Int. J. Hydrog. Energy **34**, 7368 (2009)
290 4. N.A. Kelly, T.L. Gibson, M. Cai, J.A. Spearot, D.B. Ouwerkerk, Int. J. Hydrog. Energy **35**, 892
291   (2010)
292 5. R. Matsuda, Bull. Chem. Soc. Japan **86**, 1117 (2013)
293 6. D.P. Broom, K.M. Thomas, MRS Bull. **38**, 412 (2013)
294 7. J.P. Marco-Lozar, M. Kunowsky, J.D. Carruthers, A. Linares-Solano, Carbon **76**, 123 (2014)
295 8. M.E. Casco, M. Martnez-Escandell, E. Gadea-Ramos, K. Kaneko, J. Silvestre-Albero, F. Rodriguez-
296   Reinoso, Chem. Mater. **27**, 959 (2015)

9. G. Guerra, C. Daniel, P. Rizzo, O. Tarallo, J. Polym. Sci. Part B: Polym. Phys. **50**, 305 (2012)
10. W.G. Kim, S. Nair, Chem. Eng. Sci. **104**, 908 (2013)
11. Y. Ouyang, H. Shi, R. Fu, D. Wu, Sci. Rep. **3**, 1430 (2013)
12. Y. Zheng, J. Liu, J. Liang, M. Jaroniec, S.Z. Qiao, Energy Environ. Sci. **5**, 6717 (2012)
13. M. Rose, Chem. Cat. Chem **6**, 1166 (2014)
14. N. Pal, A. Bhaumik, RSC Adv. **5**, 24363 (2015)
15. K.M. Thomas, Dalton Trans. **9**, 1487 (2009)
16. J.P. Marco-Lozar, J. Juan-Juan, F. Surez-Garca, D. Cazorla-Amors, A. Linares-Solano, Int. J. Hydrog. Energy **37**, 2370 (2012)
17. Y. Peng, V. Krungleviciute, I. Eryazici, J.T. Hupp, O.K. Farha, T. Yildirim, J. Am. Chem. Soc. **135**, 11887 (2013)
18. U. Diaz, A. Corma, Coord. Chem. Rev. **311**, 85 (2016)
19. H. Furukawa, O.M. Yaghi, J. Am. Chem. Soc. **131**, 8875 (2009)
20. S.H. Sang, H. Furukawa, O.M. Yaghi, W.A. Goddard, J. Am. Chem. Soc. **130**, 11580 (2008)
21. P. Kowalczyk, L. Solarz, D.D. Do, A. Samborski, J.M.D. MacElroy, Langmuir **22**, 9035 (2006)
22. K.L. Lim, H. Kazemian, Z. Yaakob, W.R.W. Daud, Chem. Eng. Technol. **33**, 213 (2010)
23. A. Linares-Solano, M. Jordà-Beneyto, M. Kunowsky, D. Lozano-Castelló, F. Suárez-García, D. Cazorla-Amorós, in *Carbon materials: theory and practice*. ed. by A.P. Terzyk, P.A. Gauden, P. Kowalczyk (India Research Signpost, Kerala, 2008), p. 245
24. J.P. Marco-Lozar, M. Kunowsky, F. Suarez-Garcia, J.D. Carruthers, A. Linares-Solano, Energy Environ. Sci. **5**, 9833 (2012)
25. C.M. Yang, H. Noguchi, K. Murata, M. Yudasaka, A. Hashimoto, S. Iijima, K. Kaneco, Adv. Mater. **17**, 866 (2005)
26. A. Ahmed, R. Babarao, R. Huang, N. Medhekar, B.D. Todd, M.R. Hill, A.W. Thornton, J. Phys. Chem. C **119**, 9347 (2015)
27. R. Babarao, S. Dai, D.E. Jiang, Langmuir **27**, 3451 (2011)
28. D. Beaudoin, T. Maris, J.D. Wuest, Nat. Chem. **5**, 830 (2013)
29. T. Ben, C. Pei, D. Zhang, J. Xu, F. Deng, X. Jing, S. Qui, Energy Environ. Sci. **4**, 3991 (2011)
30. T. Ben, S. Qiu, Cryst. Eng. Comm. **15**, 17 (2013)
31. K. Dhanalaxmi, R. Singuru, S. Mondal, L. Bai, B.M. Reddy, A. Bhaumik, J. Mondal, A.C.S. Sust, Chem. Eng. **5**, 1033 (2017)
32. K. Dhanalaxmi, R. Yadav, S.K. Kundu, B.M. Reddy, V. Amoli, A.K. Sinha, J. Mondal, Chem. Eur. J. **22**, 15639 (2016)
33. M. Errahali, G. Gatti, L. Tei, G. Paul, G. Rolla, L. Canti, A. Fraccarollo, M. Cossi, A. Comotti, P. Sozzani, L. Marchese, J. Phys. Chem. C **118**, 28699 (2014)
34. A. Fraccarollo, L. Canti, L. Marchese, M. Cossi, Langmuir **30**, 4147 (2014)
35. J. Fu, J. Wu, R. Custelcean, D.E. J Colloid Interface Sci. 438, 191 (2015).
36. C. Pei, T. Ben, S. Qiu, Mater. Horiz. **2**, 11 (2015)
37. G. Crini, Bioresour. Technol. **97**, 1061 (2006)
38. K.A. Krishnan, T. Anirudhan, Water SA **29**, 147 (2003)
39. Y. Sun, P.A. Webley, Chem. Eng. J. **162**, 883 (2010)
40. A.D. Leonard, J.L. Hudson, H. Fan, R. Booker, L.J. Simpson, K.J. O'Neill, P.A. Parilla, M.J. Heben, M. Pasquali, C. Kittrell, J.M. Tour, J. Am. Chem. Soc. **131**, 723 (2009)
41. R.C. Bansal, J.B. Donnet, F. Stoeckli, *Active Carbon* (Marcel Dekker, New York, 1988).
42. M.J. Illan-Gomez, A. Garcìa-Garcìia, C. Salinas-Martınez de Lecea, A. Linares-Solano. Energy Fuels **10**, 1108 (1996)
43. K. Yang, J. Peng, C. Srinivasakannan, L. Zhang, H. Xia, X. Duan, Biores. Technol. **101**, 6163 (2010)
44. G. Gatti, M. Errahali, L. Tei, M. Cossi, L. Marchese, Polymers **11**(4), 588 (2019)
45. A. Armano, S. Agnello, C 2019, 5, 67.
46. O. Beyssac, B. Goffé, C. Chopin, J.N. Rouzaud, J. Metamorph. Geol. **20**, 859 (2002)
47. L.G. Cançado, A. Jorio, E.H. Martins Ferreira, F. Stavale, C.A. Achete, R.B. Capaz, M.V.O. Moutinho, A. Lombardo, T.S. Kulmala, A.C. Ferrari, Nano Lett. **11**, 3190 (2011)
48. A.C. Ferrari, Solid State Commun. **143**, 47 (2007)
49. A. Sadezky, H. Muckenhuber, H. Grothe, R. Niessner, U. Pöschl, Carbon **43**, 1731 (2005)
50. K. Tuinstra, J.L. Koenig, J. Chem. Phys. **53**, 1126 (1970)
51. L. Bokobza, J.L. Bruneel, M. Couzi, C 1 , 77 (2015).

| Journal : **SmallExtended 11164** | Article No : **4338** | Pages : **13** | MS Code : **4338** | Dispatch : **9-12-2020** |

On the correlation between Raman spectra and structural…

52. L. Bonoldi, F. Frigerio, L. Di Paolo, A. Savoini, D. Barbieri, D. Grigo, Energy Fuels **32**, 8955 (2018)
53. S. Claramunt, A. Varea, D. López-Díaz, M.M. Velázquez, A. Cornet, A. Cirera, J. Phys. Chem. C **119**, 10123 (2015)
54. D.L. Henry, I. Jarvis, G. Gillmore, M. Stephenson, J.F. Emmings, Int. J. Coal Geol. **191**, 135 (2018)
55. C. Hu, S. Sedghi, A. Silvestre-Albero, G.G. Andersson, A. Sharma, P. Pendleton, F. Rodríguez-Reinoso, K. Kaneko, M.J. Biggs, Carbon **85**, 147 (2015)
56. Y. Kouketsu, T. Mizukami, H. Mori, S. Endo, M. Aoya, H. Hara, D. Nakamura, S. Wallis, Island Arc **23**, 33 (2014)
57. K.N. Kudin, B. Ozbas, H.C. Schniepp, R.K. Prud'homme, I.A. Aksay, R. Car, Nano Lett. **8**, 36 (2008)
58. D. López-Díaz, M. López-Holgado, J.L. García-Fierro, M.M. Velázquez, J. Phys. Chem. C. **121**, 20489 (2017)
59. N.K. Lünsdorf, I. Dunkl, B.C. Schmidt, G. Rantitsch, H. von Eynatten, Geostand. Geoanalytical Res. **38**, 73 (2013)
60. G. Rajender, P.K. Giri, J. Mater. Chem. C **4**, 10852 (2016)
61. B. Sauerer, P.R. Craddoc, M.D. Aljohani, K.L. Alsamadony, W. Abdallah, Int. J. Coal Geol. **173**, 150 (2017)
62. R. Sparkes, N. Hovius, A. Galy, R.V. Kumar, J.T. Liu, Appl. Spectrosc. **67**, 779 (2013)
63. J.S. Roh, Carbon Lett. **9**, 127 (2008)
64. D. Lozano-Castello, J.M. Calo, D. Cazorla-Amoros, A. Linares-Solano, Carbon **45**, 2529 (2007)

Author Query Form

Please ensure you fill out your response to the queries raised below and return this form along with your corrections

Dear Author

During the process of typesetting your article, the following queries have arisen. Please check your typeset proof carefully against the queries listed below and mark the necessary changes either directly on the proof/online grid or in the 'Author's response' area provided below

Query	Details Required	Author's Response
AQ1	As per springer journal style corresponding author is must. since we have no mail ID for the corresponding author. we have retained the mail ID and changed the corresponding author's mail ID. Kindly check and confirm.	
AQ2	Kindly provide complete information for the references [35, 45, 51].	
AQ3	Reference [64] was provided in the reference list; however, this was not mentioned or cited in the manuscript. As a rule, if a citation is present in the text, then it should be present in the list. Please provide the location of where to insert the reference citation in the main body text. Kindly ensure that all references are cited in ascending numerical order.	
AQ4	please provide us the author biography photos.	